Published in final edited form as:
Eur J Oral Sci. 2013 December ; 121(6): 600–609. doi:10.1111/eos.12081.

Structure-activity relationship of human bone sialoprotein peptides

Bruce E. Rapuano[a] and **Daniel E. MacDonald**[a,b,c]

[a] Hospital for Special Surgery affiliated with the Weill Medical College of Cornell University, 535 East 70th Street, New York, NY 10021, USA

[b] James J. Peters VA Medical Center, 130 West Kingsbridge Road, Bronx, NY, 10468, USA

[c] Langmuir Center for Colloids and Interfaces, Columbia University, 911 S.W. Mudd Building, Mail Code 4711, 500 West 120th Street, New York, NY 10027, USA

Abstract

In the current study, the relationship between the structure of the RGD-containing human bone sialoprotein (hBSP) peptide 278-293 and its attachment activity toward osteoblast-like (MC3T3) cells was investigated. This goal was accomplished by examining the comparative cell attachment activities of several truncated forms of peptide 278-293. Computer modeling of the various peptides was also performed to assess the role of secondary structure in peptide bioactivity. The elimination of the tyrosine-278 at the N-terminus resulted in a more dramatic loss of cell attachment activity compared to the removal of either tyrosine-293 or the arg-ala-tyr (291-293) tripeptide. Although the replacement of the RGD (arg-gly-asp) peptide moiety with peptide KAE (lys-ala-glu) resulted in a dramatic loss of cell attachment activity, a peptide containing RGE (arg-glyglu) in place of RGD retained 70-85 % of the parental peptide's attachment activity. These results suggest that the N-terminal RGD-flanking region of hBSP peptide 278-293, in particular the tyrosine-278 residue, represents a second cell attachment site that stabilizes the RGD-integrin receptor complex. Computer modeling also suggested that a β-turn encompassing RGD or RGE in some of the hBSP peptides may facilitate its binding to integrins by increasing the exposure of the tripeptide. This knowledge may be useful in the future design of biomimetic peptides which are more effective in promoting the attachment of osteogenic cells to implant surfaces in vivo.

Keywords

biomimetic; extracellular matrix; RGD peptide; integrins; osteoblasts

Titanium and titanium alloys have been employed in orthopedics and dental implants due to their biocompatibility (1,2). However, implant loosening and failure is still a significant problem with a sizeable percentage of hip arthroplasties. In fact, 25% of hip replacement surgeries were revisions due to previous implant failure (3). Despite the reported long-term

To whom reprint requests should be sent : Daniel E. MacDonald Hospital for Special Surgery 535 East 70th Street New York, NY 10021, USA. dem14@columbia.edu.

Conflicts of interest. The authors do not have a financial relationship with the organization that sponsored the research. The authors declare that they have no conflicts of interest.

predictability of dental implants (4,5), failures do occur in 10% of cases within a 5-yr period (6). The survival rates decrease to 71-83.5% over a 3.5-6 yr period for dental implants placed in previously failed implant sites (7,8). Evidence suggests that the quality and quantity of bone formation at the implant-skeletal interface are important to insure long-term success (9). The biointegration of implant materials in an osteotomy site is largely dependent on the activity of bone-forming cells (or their precursors) from the host tissues (10). Implant surface modifications that increase surface coverage by bone have been shown to increase implant-bone interface strength as well as stimulate the capacity (11) of attached osteoblasts to differentiate and synthesize an extracellular matrix (12). Moreover, osteoblasts have been shown to attach in vivo to dental implant surfaces within 24 h. of insertion and produce a collagenous matrix (13). These findings suggest that the efficient recruitment and attachment of osteoblasts to the implant surface will accelerate and strengthen bone integration. Therefore, novel biomimetic materials should be designed to support and enhance osteoblast attachment.

To prevent implant failure, a variety of methods have been explored, including the use of extracellular matrix proteins (ECM) or bioactive attachment peptides from these proteins to facilitate the attachment of osteogenic cells to the implant surface. Our laboratory has studied the effects of ECM proteins such as fibronectin or human bone sialoprotein (hBSP) or hBSP peptides, following their non-covalent adsorption to implant surfaces, on osteoblast attachment and function (14-23). A key binding domain in ECM proteins for osteoblast integrin receptors is the RGD tripeptide (24-26). RGD is present in a number of ECM proteins, including fibronectin (27) and BSP (28-29). RGD-containing peptides have been shown to promote early bone growth and matrix mineralization *in vivo* (30,31). Other studies have shown that fibronectin added to implant materials is able to attach to bone cells *in vivo* and promote bone formation around implant materials (32,33). Our laboratory has also demonstrated a clear relationship between the capacity of fibronectin coated on implant materials to increase osteoblast attachment, function and biomineralization *in vitro* (14-23) and the stimulatory effects of fibronectin coatings on implant osseointegration *in vivo* (34). Therefore, even though inflammatory and other cells are present at the implant-skeletal interface immediately after placement (35), osteoblasts, which have been shown to rapidly attach (within 24 h) to implant materials (13), are likely to enhance their osseointegration in response to biomimetic RGD peptides or protein coatings.

A number of studies have shown that the spatial conformation of RGD peptides influences their biological activities (36-38). Moreover, evidence suggests that peptide domains exhibiting the more extended beta-sheet conformation, which are less subject to intrachain binding than tighter alpha-helical structures, are involved in the RGD-dependent interactions of cell attachment molecules (28,39) or fibronectin (40) with cell integrin receptors. Differences in the conformation of BSP peptides have been predicted based on amino acid composition (28,41). In order to assess the contribution of secondary structure to the optimal design of attachment-promoting peptides, we have previously examined the osteogenic cell attachment properties (16) of a number of RGD-containing hBSP peptides which, based on their amino acid composition, may promote a beta-sheet conformation within the local PRGD (pro-arg-gly-asp) domain. Consideration was given, in the peptide design, to the

demonstrated effectiveness of glycine and serine residues as destabilizers of alpha-helical peptide organization (42). The relative contributions of RGD and non-RGD domains to peptide biological activity toward osteogenic cells was also examined. We previously demonstrated that the BSP peptides P3 (residues 278-293) and P4 (278-302), each containing RGD at positions 286-288, were equivalent in attachment potency and 1-2 orders of magnitude greater in potency than peptide P2 (281-290). These findings suggested that non-RGD regions 278-280 and 291-293 are important for cell attachment, whereas (since BSP peptides 278-302 and 278-293 were equivalent in potency) the tyrosine-rich 294-302 region was not necessary for cell attachment (16).

In the current study, we have attempted to further elucidate the structure-activity relationship of hBSP peptide 278-293 by comparing the attachment effects of structurally related isoforms of this peptide that were progressively truncated in regions 278-280 and 291-293. Also, to evaluate the previously postulated role of tyrosines in secondary cell attachment sites outside the RGD domain (28), we have measured the bioactivities of a number of peptide variants from which tyrosines flanking the RGD domain were omitted. Blocking experiments with a soluble RGD peptide and anti-integrin antibodies, respectively, were performed to assess the role of RGD in integrin binding and identify the major integrin isoforms responsible for cell attachment to the hBSP peptides. In addition, the role of tyrosine sulfation of hBSP peptides in cell attachment and the influence of peptide secondary structure, predicted by computer modeling, on attachment activity were also investigated.

Materials and Methods

Ten BSP peptides described in Figs. 1 and 2 were used for this study. The comparative structures of six truncated forms of peptide hBSP peptide 278-293 used in this study, including peptides 281-290 (P2), 281-293 (DB1), 278-290 (DB2), 279-293 (DB3), 278-292 (DB4) and 279-292 (DB5), are shown in Fig. 1A. The structures of three modified variants of peptide 278-292, which included the replacement of aspartic acid with glutamic acid at residue 288 (DB4-E), the replacement of arginine-glycine-aspartic acid at 286-288 with lysine-alanine-glutamic acid (DB4-KAE) and the sulfation of tyrosines 278 and 290 (DB4-sulfate), are shown in Figure 1B. The attachment effects of peptides 278-293 (P3) and 281-290 (P2) have been previously reported (16). Peptides were synthesized by SynPep (Dublin, CA, USA) using FMOC chemistry to a purity of 90-95% based on high performance liquid chromatography (HPLC) and amino acid analysis. Newborn calf serum (NCS), fetal bovine serum FBS and cell culture media were obtained from Gibco Laboratories (Grand Island, NY, USA). Rat anti-mouse α_v (CD51) and $\alpha_5\beta_1$ monoclonal antibodies were obtained from Chemicon / Millipore (Billerica, MA, USA). RGD peptide, bovine serum albumin (BSA ; Fraction V; essentially fatty acid-free) and *p*-nitrophenol-*N*-acetyl-β-D-glucoseaminide were from Sigma (St. Louis, MO, USA). Tissue culture flasks (75 cm^2), 96-well tissue culture plates and non-tissue culture treated plates were obtained from Laboratory Disposable Products (North Haledon, NJ, USA).

Computer modeling of hBSP peptides

The I-TASSER server for protein structure and function predictions was used to obtain high-quality predictions of secondary structure of hBSP peptides from their amino acid sequences (43,44). TM-align was used to estimate the accuracy of the top five full-length models predicted by the I-TASSER server. TM-align is a computer algorithm for protein structure alignment using dynamic programming and TM-score rotation matrix. The program provides an averaged TM-score that compares the global structural similarity of the full-length model created for the target sequence with that of each of the top ten protein templates that were used to generate the model. The value of TM-score lies in (0,1). In general, a comparison of TM-score < 0.2 indicates that there is no similarity between two structures; a TM-score > 0.5 means the structures (the template and target sequence model) share the same fold (43,44).

Cell culture

MC3T3-E1, an osteoblast-like cell line cloned from a mouse calvarium, was kindly provided by Dr. M. Kumegawa, Josai Dental University (Sakado, Japan). MC3T3-E1 cells were cultured in MEM (Modified Eagle's Medium) -α with 5% FBS and 5% NCS. MG63 (ATCC) human osteoblast-like cells were cultured in Modified Eagles Medium + nonessential amino acids (MEM+ NEAA) with heat-inactivated 10% FBS as previously described (17).

Precoating of 96-well plates with BSP peptides

To examine the effect of BSP peptides on cell attachment, 96-well non-tissue culture polystyrene plates were coated with concentrations of peptide, washed, aftercoated with BSA and washed as previously described (16). These plates were then employed for the cell attachment and RGD-inhibition studies described below. Uncoated non-tissue culture polystyrene plates served as a control for these studies.

Peptide-induced cell attachment

Cells were plated at 30,000 cells/well in serum-free growth medium for 2-h at 37ºC in peptide precoated 96-well non-tissue culture plates. After washing the plates three times with PBS, cell attachment was quantified using an assay of hexosaminidase activity (45) as previously described (16).

Inhibition of cell attachment by pre-saturation of integrin receptors with RGD or anti-integrin antibodies

In order to determine whether or not RGD-binding integrin receptors played a role in the cell attachment activities of the hBSP peptides studied, MC3T3 cells were exposed in microcentrifuge tubes for 30 minutes to 1 – 500 μM of the tripeptide RGD or 1:500 to 1:25 dilutions of an anti-α_v or anti-$\alpha_5\beta_1$ integrin antibody in serum-free media with 0.1% BSA. Both the anti-alpha V and anti-alpha-5, beta-1 monoclonal antibodies have been shown to block their respective integrin receptors and the adhesion of cells mediated by these receptors in the mouse, although cross-reactivity with other integrins was not tested (Chemicon / Millipore, www.millipore.com). FBS was added to the tubes at 10% v/v and

the cells were pelleted at 600 X g for 5 min., washed twice with serum-free media and plated at a density of 30,000 cells/well in the peptide precoated 96-well non-tissue culture polystyrene plate. After a 2-h incubation at 37°C, the plates were washed three times with PBS, and cell attachment was quantified by measuring hexosaminidase activity (45) as described above.

Measurements of peptide adsorption to 96-well plates

In order to measure their adsorption to polystyrene, 96-well nontissue culture plates were coated with peptides and washed as described above. The amount of peptides in micrograms which remain adsorbed was then quantified in the same 96-well plate by protein assay using the Micro BCA Protein Assay Reagent kit (Pierce, Rockford, IL, USA) and measured at a wavelength of 562 nm. Stock solutions of peptides at known concentrations were used as standards.

Statistical analysis

All values are presented as mean ± SEM for all control and experimental (N= total number of independent cultures). For any given experiment, individual data is expressed as % control (control defined at 100%). Statistical comparisons were performed using a paired Student t-test with the alpha level for each test set at 0.05.

Results

MC3T3 cells were plated on 96-well nontissue culture plates precoated overnight with the indicated solution phase concentrations of hBSP peptides so that the comparative cell attachment effects of several truncated forms of hBSP peptide 278-293 could be evaluated (Fig. 2). The cell attachment activities of six truncated forms of hBSP peptide 278-293 (P3), each containing the core sequence glu-asn-gly-glu-pro-arg-gly-asp-asn-tyr at positions 281-290 (Fig. 1), are shown in Fig. 2. Of this group, only peptides 279-293 (DB3), lacking the N-terminal tyrosine, and 281-290 (P2), lacking both the tripeptide tyr-glu-ser (Y-E-S) from the N-terminus and the tripeptide arg-ala-tyr (R-A-Y) from the C-terminus (Fig. 1), failed to induce a statistically significant increase in MC3T3 cell attachment at any of the coating phase concentrations tested (Fig. 2). The latter peptide has already been shown to be comparatively inactive as a cell attachment stimulus among a structurally related group of hBSP peptides including P3 (16).

hBSP peptides 278-290 (DB2), lacking residues arg-ala-tyr from the C-terminus (Fig. 1), and 278-292 (DB4), lacking only the C-terminal tyrosine (Fig. 1), demonstrated the greatest maximal stimulation of attachment of all of the truncated forms of the native peptide (P3) tested (Fig. 2). DB4 and DB2 each demonstrated a stimulatory effect on cell attachment compared to uncoated wells that was statistically significant ($P < 0.001$ and 0.007, respectively) at every [peptide] coating concentration tested (Fig. 2). Peptide 278-292 (DB4) was also the only member of this group of truncated hBSP peptides which appeared to manifest a full retention of the parental peptide's integrin receptor affinity, with both peptides demonstrating half-maximal effects at approximately 1 μM of peptide solution phase concentration (Fig. 2). In contrast, peptides 281-293 (DB1) and 279-292 (DB5) only

increased cell attachment maximally to 150-300 % of control levels even when tested at solution phase concentrations as high as 50 – 200 μM (Fig. 2). The number of attached cells measured in the presence of DB4 was found to be statistically greater ($P < 0.04$) than that measured in the presence of DB1, DB3, DB5 or P2 at each corresponding solution phase concentration tested (Fig. 2).

For each of the hBSP peptides tested, the number of attached cells was also plotted vs. the adsorbed peptide's surface concentration measured by protein assay (Fig. 2B). Maximal levels of 6 – 8 nmoles (9 to 12 μg) of peptide per cm^2 were observed to adsorb to individual wells in the nontissue culture plate. When compared over an equivalent range of surface concentrations (Fig. 2B), the peptides demonstrated the same relative potencies for the stimulation of cell attachment that was observed when cell attachment was plotted against the [peptide] in the coating solution : P3 = DB4 > DB2 > DB1 > DB5 > DB3 = P2 (Fig. 2). These findings indicate that the wide dissimilarities observed between these seven hBSP peptides in their cell attachment potencies are not attributable to the modest differences found in their adsorption to the polystyrene cultures plates (unpublished findings).

The effects of hBSP peptides on the attachment of cells from the MG63 human osteogenic sarcoma line were also investigated. MG63 cells display many of the characteristics of differentiated osteoblasts (46). When MG63 cell attachment to hBSP peptides was measured, peptides P3 and P2 exhibited the same relative potencies (Fig. 3) that were observed for MC3T3 cell attachment (Fig. 2) over an equivalent range of peptide coating solution or surface concentrations. P3 promoted statistically significant increases in the number of attached MG63 cells at every coating concentration compared to control or P2-coated wells. However, there were no significant differences between the numbers of MGG3 and MC3T3 cells that attached to either peptide as a percentage of control cell attachment (Fig. 3). The maximal percentage increases in the attachment of MG63 cells promoted by peptides DB4, DB2, DB1 and DB3 over the range of surface concentrations shown for P3 in Fig. 3 were 731 ± 100 %, 422 ± 41 %, 371 ± 21 % and 228 ± 14 % (mean ± S.E ; N = at least 6). Therefore, the hBSP peptides manifested the same order of potency for the stimulation of MG63 cell attachment : P3 = DB4 > DB2 > DB1 > DB3 = P2 that was observed for MC3T3 cell attachment (Fig. 2).

Our laboratory has shown that the attachment of MC3T3-E1 cells to hBSP peptides, including P3, was significantly inhibited by solution phase RGD in a concentration dependent manner (16). Following the pre-incubation of cells with RGD in solution phase, peptides DB1 and DB2 each manifested a similar sensitivity to the inhibitory effects of RGD on MC3T3 cell attachment compared to P3 (Fig. 4A). All three peptides retained similar residual MC3T3 cell attachment activities (10-20 % of control) at an RGD concentration of 500 μM (Fig. 4A). DB4 exhibited a sensitivity to RGD which mirrored that of the other hBSP peptides, displaying 28 ± 10 % and 14 ± 9 %, respectively, of its cell attachment activity when cells were preincubated with 1 or 500 μM RGD (mean ± S.E ; N = 5-6).

The pre-incubation of cells with an antibody to $\alpha_v\beta_3$ integrin was found to decrease the number of cells that attached to a P3 coating (10 μM coating concentration), reducing cell attachment by 45 ± 4 % (N = 5) at an antibody dilution of 1 : 25. When compared at the

same dilution, the pre-incubation of cells with an antibody to $\alpha_5\beta_1$ integrin was found to decrease the number of cells that attached to a P3 coating by 29 ± 2 % (N = 12) (Fig. 4B).

When the attachment activity of DB4 was compared with that of a structural variant of the peptide modified by the sulfation of tyrosines 278 and 290 (DB4-sulfate), no differences were found between the parental and modified molecules in their potencies or maximal effects (unpublished findings). DB4-sulfate demonstrated a stimulatory effect on cell attachment compared to uncoated wells (0 μM DB4-sulfate) that was statistically significant ($P < 0.04$) at every coating solution concentration tested. Furthermore, no statistically significant differences were found between the number of attached cells measured in the presence of DB4-sulfate and that measured in the presence of DB4 at each concentration tested (unpublished findings).

The importance of the RGD region in cell attachment to the hBSP peptides was evaluated by replacing the glutamic acid in the RGD sequence of DB4 with aspartic acid (changing RGD to RGE) and comparing the modified peptide's cell attachment activity to that of the native peptide. The modified peptide (DB4-E) appeared to retain the potency of the parental molecule, promoting a concentration-dependent increase in MC3T3 cell attachment (Fig. 5). DB4-E induced an increase in cell attachment compared to control that was statistically significant ($P < 0.001$) at every concentration tested (Fig. 5). However, when compared over an equivalent range of surface concentrations, the RGE variant manifested a loss of 15-30 % of the cell attachment activity of DB4 (Fig. 5B). The lower relative potency observed for DB4 when cell attachment was plotted against solution [peptide] is attributable to the generally much lower levels of surface adsorption found for the native peptide compared to its RGE variant at coating concentrations higher than 1 μM (Fig. 6). Notably, the levels of cell attachment to DB4 progressively increased from 380 % of control at a 1 μM coating solution to 540 %, 590 %, 670 % and 710 % at 10, 50, 100 and 200 μM (Fig. 2), respectively. Therefore, it is unlikely that the adsorption of DB4 to the plastic became saturated at 1 μM (Fig. 6) such that additional adsorption at higher coating concentrations would reflect peptide-peptide interactions.

To determine if the attachment function of DB4 was entirely independent of the tripeptide RGD sequence, the arg-gly-asp region was completely replaced with lys-ala-glu (changing RGD to KAE) and the relative attachment activities of the native (DB4) and modified (DB4-KAE) peptides were compared. In contrast to DB4-E, the KAE-containing peptide retained little of the attachment efficacy of DB4 even when compared at the same surface concentrations (Fig. 5B). DB4-KAE induced an increase in cell attachment compared to control that was statistically significant ($P < 0.003$) at every concentration tested (Fig. 5). However, at its peak effect, DB4-KAE only increased the number of attached cells to a maximum of 235 ± 21 % of control (Fig. 5).

To assess the potential role of secondary structure in the cell attachment activities of the hBSP peptides, the I-TASSER server was used to obtain high-quality predictions of secondary structure of hBSP peptides from their amino acid sequences. I-TASSER-based computer modeling indicated that all of the hBSP peptide primary structures which contained the tyrosine-293 residue (P3, DB1 and DB3) favored an alpha-helix conformation

from 287G to 292A (Fig. 7, Table 1). All of the peptide structures, including those of P2, DB2, DB4, DB4-E, DB4-KAE and DB5, from which tyrosine-293 was omitted no longer favored this particular alpha helix conformation (Fig. 7, Table 1). Notably, three of the peptide structures (DB4, DB4-E and DB5) from which tyrosine-293 was omitted instead favored a beta hairpin turn affecting at least two of the three residues present in the RGD or RGE domains (Table 1). Each of the secondary structure models shown in Table 1 represent one of the top 1-2 models of the 5 best models predicted by the I-TASSER server. TM-scores for all of the predicted secondary structures shown in Table 1 (except that for DB4-E and DB5) were at least 0.5.

Discussion

Our study has examined the role of amino acids, principally tyrosines, that flank the RGD sequence (from 286 to 288) in the cell attachment activity of BSP peptide 278-293 (P3). Our results show that the simple deletion of tyrosine-278 from peptide 278-293 to yield DB3 resulted in a substantial loss of cell attachment activity which was more dramatic than that caused by the deletion of the entire tripeptide Y-E-S (peptide 278-280) to yield DB1. In contrast, the elimination of tyrosine-293 from P3 or DB3 to yield DB4 or DB5, respectively, resulted in little or no loss of cell attachment activity. Although the removal of the R-A-Y tripeptide (291-293) from P3 to form DB2 caused a significant reduction in cell attachment activity, this was much less than that produced by the deletion of tyrosine-278. These results suggest that other binding sites in hBSP peptide P3 outside of the RGD domain participate in cell attachment. Our findings also suggest a greater role for tyrosine-278 in the peptide's cell attachment activity compared to either tyrosine 293 or the entire C-terminal R-A-Y. It has been suggested that the sulfation of tyrosines in hBSP peptides may stabilize the conformation of an integrin binding domain (43). However, we found that the sulfation of tyrosines in DB4 had no effect on cell attachment activity, indicating that other factors are involved in the effects of tyrosine-278 on cell attachment.

We found that hBSP peptides P3 and DB4 promoted a several-fold enhancement in the level of MC3T3 osteoprogenitor cell attachment at a coating concentration as low as 1 μM (Fig. 2). In comparison, a recombinant hBSP peptide (258-317) containing tyrosine-rich stretches in the N-terminal region and C-terminal regions flanking the RGD domain was found to stimulate the attachment of MC3T3 cells at a concentration of 55 μM (28). In the latter study, S_{TUBBS} et al. proposed a model in which a (tyrosine-rich) second attachment site would bind integrins close to the RGD-binding pocket due to its proximity to the RGD sequence. The authors further postulated that in inhibition experiments with a soluble GRGDS peptide the displacement of the RGD in peptide 258E to 317Q from the integrin receptor's RGD-binding pocket by the GRGDS peptide also destabilized the binding of the tyrosine-rich second site to the integrin receptor (28). If this model were true, then the RGD and non-RGD tyrosine-rich attachment sites may interact synergistically by coordinately stabilizing the peptide-integrin receptor complex. A similar model, in which the RGD tripeptide and a second synergy attachment site located at the N-terminus of hBSP peptide P3 bind in a cooperative manner to integrin, may explain why tyrosine-278 is so central to the cell attachment activity of this latter hBSP peptide.

The integrin-binding capacity of the RGD sequence is highly influenced by its secondary structure and conformation (47). Some amino acid residues have a strong beta-sheet or alpha-helix forming capacity while others destabilize alpha helix structures (42). Therefore, some of the differences in cell attachment observed between the various hBSP peptides studied might be attributable to changes in secondary structure that result from the exclusion or substitution of specific residues. Although most RGD-containing proteins lack a stable conformation at the RGD site (48-49), short RGD peptides demonstrate the tendency to form a β-turn in solution (50). Based on methods for predicting secondary structure (42), it has been suggested that integrin-binding polypeptides such as fibronectin are likely to interact with the receptor via a hydrophilic loop formed by a β-turn containing RGD (27). The hydrophilic loop at the protein's surface would be more available for interactions with the cell surface than regions of the protein with a more extended (as opposed to compact) secondary structure (27). Notably, the elimination of the C-terminal tyrosine-293 from P3 yielded a primary structure (DB4) that favored a β-turn conformation in the RGD or in the RGE domain of DB4-E. The finding that either DB4 and DB4-E retained much of the cell attachment activity of the parental peptide (P3) suggests that this β-turn in RGD or RGE may compensate for the loss of any contribution from the C-terminal tyrosine to integrin binding. In DB4-E, the peptide-integrin complex could have been stabilized partly by the effects of a β-turn on the exposure of the RGE tripeptide and partly by the binding of a second attachment site (containing the tyrosine-278) close to the RGD-binding pocket (28), as discussed above. The adsorption of the peptides to the surface most likely affects the possible conformations that the peptides can or will acquire. However, limited peptide-surface interactions may still permit significant flexibility in the RGD tripeptide and the formation of a β turn in this domain that can influence the peptide's binding to cell receptors.

Notably, a tyrosine-rich hBSP peptide (258E to 317Q) in which RGD was replaced with KAE was shown by Stubbs et al. (28) to retain attachment activity. Computer modeling performed in the current study indicates that primary structure of this latter peptide does favor a β-turn for the KAE tripeptide. In contrast, computer modeling and cell attachment results suggests that the loss of a structure that favors a β-turn in the KAE variant of peptide DB4 (Table 1) may have reduced the exposure of this latter tripeptide to the degree that it can no longer participate in integrin binding. The results reported by Stubbs et al. (28) together with our results with the KAE variant of DB4 further suggest that the tyrosine-containing N-terminal domain in the latter peptide can function well to promote cell attachment only in the presence of either an intact RGD or a β-turn at sequence 286-288. Conversely, the very low cell attachment activity and predicted secondary structure (Table 1) of hBSP peptide P2 (281-290) suggests that the RGD domain functions poorly in the absence of both a β-turn (that may be favored by the RGD tripeptide alone) and the N-terminal tyrosine. Alternatively, peptide 281-290 may fold into a more compact structure than that predicted by computer modeling, thereby completely shielding the RGD domain and rendering it inaccessible to cell receptors.

Although MC3T3 cells express several integrins, including $\alpha_2\beta_1$, $\alpha_3\beta_1$, $\alpha_4\beta_1$, $\alpha_5\beta_1$, $\alpha_6\beta_1$, $\alpha_v\beta_1$ and $\alpha_v\beta_3$, blocking with inhibitory antibodies has demonstrated that $\alpha_5\beta_1$ and $\alpha_v\beta_3$ integrins are the major integrin receptors in this cell line (51). A number of findings indicate that BSP probably binds more effectively to $\alpha_v\beta_3$ integrin than to other integrins including

$\alpha_5\beta_1$ (52-57). In contrast, it has been shown that $\alpha_5\beta_1$ integrins provide the dominant mechanism of MC3T3 cell adhesion to fibronectin (51). We have found that an anti-$\alpha_v\beta_3$ integrin antibody blocked the attachment of MC3T3 cells to the hBSP peptide P3 (278-293) by 45 % whereas an anti-$\alpha_5\beta_1$ antibody only decreased MC3T3 cell attachment to the hBSP peptide by 29 %. Therefore, findings in the current study that an antibody to $\alpha_V\beta_3$ integrin decreased the number of attached cells more than an antibody directed against $\alpha_5\beta_1$ integrin suggests that the attachment of MC3T3 cells was primarily mediated by hBSP peptides, not fibronectin produced in culture by the cells. Also, since each antibody inhibited cell attachment to hBSP peptide P3 by only 20-40 %, integrins other than $\alpha_5\beta_1$ and $\alpha_V\beta_3$ may contribute to the total levels of attachment measured. Notably, since RGD was found to block 80-90 % of the attachment of cells to the hBSP peptides examined in the current study, nearly all of the cell binding to the peptides appears to be integrin-mediated.

It is possible that tyrosine-278 in hBSP peptide 278-292 binds to a different receptor than the RGD domain. However, the close proximity of the two sites to one another and the dramatic losses of cell attachment activity that were observed when attachment was blocked by solution phase RGD, tyrosine-278 was eliminated or RGD was replaced by KAE all strongly suggest that the RGD tripeptide and tyrosine-278 bind cooperatively to the same receptor. A number of laboratories (30-33) have demonstrated the potential utility of biomimetic protein and peptide coatings in promoting the osseointegration of implant materials. The current study has demonstrated that the osteoblast cell attachment activity of hBSP RGD-containing peptides may be significantly improved by including tyrosine residues in the N-terminal region flanking the RGD domain that may act in synergy with the tripeptide. This information can be exploited in the design of novel biomimetic peptide coatings of implant materials with enhanced effects on osseointegration due to a greater stimulation of osteoblast attachment, differentiation and biomineralization. Notably, since we have shown that fibronectin binds rapidly and irreversibly to TiO2 (15), we would expect that smaller peptides would at least remain adsorbed to implant surfaces long enough to stimulate the attachment of osteoblasts, which has been shown to occur within 24 hours in vivo (13). Also, we have shown that fibronectin coatings of a titanium alloy implant material stimulate osteoblast attachment, function and biomineralization *in vitro* (14-23) and early bone formation around the implant and enhanced implant-skeleton mechanical bonding strength *in vivo* at 6 weeks following implantation (34). These findings suggest that if stimulatory effects of hBSP peptide coatings on osteoblast activity and osteogenesis can be produced *in vivo* they are likely to lead to longterm effects on implant stability.

Acknowledgments

This work was supported by VA Merit Grant # 2894-005 and by Grant Number NIH RO1 DE017695 (both awarded to DEM). This material is also the result of work supported with resources and the use of facilities at the James J. Peters VA Medical Center, Bronx, New York. This investigation was also conducted at the HSS research facility constructed with support of Grant C06-RR12538-01 from the National Center for Research Resources, NIH. The authors wish to acknowledge the technical assistance of Christina Silva, Keith Tachibana and Kyle Hackshaw.

References

1. LARSSON G, THOMSEN P, ARONSSON BO, RODAHL M, LAUSMAA J, KASEMO B, ERICSON LE. Bone response to surface-modified titanium implants: studies on the early tissue

response to machined and electropolished implants with different oxide thicknesses. Biomaterials. 1996; 17:605–616. [PubMed: 8652779]

2. TENGVALL P, LUNDSTROM I. Physico-chemical considerations of titanium as a biomaterial. Clinical Materials. 1992; 9:115–134. [PubMed: 10171197]
3. WEBSTER TJ. Nanophase ceramics as improved bone tissue engineering materials. Am Ceram Soc Bull. 2003; 82:1–8.
4. ADELL R, ERIKSEN B, LEKHOLM U, BRANEMARK PI, JEMT T. A long-term follow-up study of osseointegrated implants in the treatment of totally edentulous jaws. Int J Oral Maxillofac Implants. 1990; 5:347–359. [PubMed: 2094653]
5. ADELL R, LEKHOLM U, ROCKLER B, BRANEMARK PI. A 15-year study of osseointegrated implants in the treatment of the edentulous jaw. Int J Oral Surg. 1981; 10:387–416. [PubMed: 6809663]
6. HARDT CR, GRONDAHL K, LEKHOLM U, WENNSTROM JL. Outcome of implant therapy in relation to experienced loss of periodontal bone support: A retrospective 5-year study. Clin Oral Implants Res. 2002; 13:488–494. [PubMed: 12453125]
7. GROSSMAN Y, LEVIN L. Success and survival of single dental implants placed in sites of previously failed implants. J Periodontol. 2007; 78:1670–1674. [PubMed: 17760534]
8. MACHTEI EE, MAHLER D, OETTINGER-BARAK O, ZUABI O, HORWITZ J. Dental implants placed in previously failed sites: survival rate and factors affecting the outcome. Clin Oral Implants Res. 2008; 19:259–264. [PubMed: 18177430]
9. JOHANSSON P, STRID KG. Assessment of bone quality from cutting resistance during implant surgery. Int J Oral Maxillofac Implants. 1994; 9:279–288.
10. LEGEROS RZ, CRAIG RG. Strategies to affect bone remodeling : osteointegration. J Bone Miner Res. 1993; 8:S583–S596. [PubMed: 8122530]
11. THOMAS KA, KAY JF, COOK SD, JARCHO M. The effect of surface macrotexture and hydroxyapatite coating on the mechanical strengths and histologic profiles of titanium implant materials. J Biomed Mater Res. 1987; 21:1395–1414. [PubMed: 3429474]
12. COOPER LF. A role for surface topography in creating and maintaining bone at titanium endosseous implants. J Prosth Dent. 2000; 84:522–534.
13. MEYER U, JOOS U, MYTHILI J, STAMM T, HOHOFF A, FILLIES T, STRATMAN U, WIESMANN HP. Ultrastructural characterization of the implant/bone interface of immediately loaded dental implants. Biomaterials. 2004; 25:1959–1967. [PubMed: 14738860]
14. MACDONALD DE, MARKOVIC B, ALLEN M, SOMASUNDARAN P, BOSKEY AL. Surface analysis of human plasma fibronectin adsorbed to commercially pure titanium materials. J Biomed Materials Res. 1998; 41:120–130.
15. MACDONALD DE, DEO N, MARKOVIC B, STRANICK M, SOMASUNDARAN P. Adsorption and dissolution behavior of human plasma fibronectin on thermally and chemically modified titanium dioxide particles. Biomaterials. 2002; 23:1269–1279. [PubMed: 11791930]
16. RAPUANO BE, WU C, MACDONALD DE. Osteoblast-like cell attachment to bone sialoprotein peptides. J Orthop Res. 2004; 22:353–361. [PubMed: 15013096]
17. MACDONALD DE, RAPUANO BE, DEO N, STRANICK M, SOMASUNDARAN P, BOSKEY AL. Thermal and chemical modification of titanium-aluminum-vanadium implant materials: effects on surface properties, glycoprotein adsorption, and MG63 cell attachment. Biomaterials. 2004; 25:3135–3146. [PubMed: 14980408]
18. MACDONALD DE, RAPUANO BE, SCHNIEPP HC. Surface oxide net charge of a titanium alloy : comparison between effects of treatment with heat or radiofrequency plasma glow discharge. Colloids Surf, B. 2011; 82:173–181.
19. RAPUANO BE, MACDONALD DE. Surface oxide net charge of a titanium alloy: Modulation of fibronectin-activated attachment and spreading of osteogenic cells. Colloids Surf, B. 2011; 82:95–103.
20. RAPUANO BE, LEE JJ, MACDONALD DE. Titanium alloy surface oxide modulates the conformation of adsorbed fibronectin to enhance its binding to α5β1 integrins in osteoblasts. Eur J Oral Sci. 2012; 120:185–194. [PubMed: 22607334]

21. RAPUANO BE, HACKSHAW KM, SCHNIEPP HC, MACDONALD DE. Effects of coating a titanium alloy with fibronectin on the expression of osteoblast gene markers in the MC3T3 osteoprogenitor cell line. J Oral Maxillofac Implants. 2012; 27:1081–1090.
22. RAPUANO BE, HACKSHAW K, MACDONALD DE. Heat or radiofrequency glow discharge pretreatment of a titanium alloy stimulates osteoblast gene expression in the MC3T3 osteoprogenitor cell line. J Periodontal Implant Sci. 2012; 42:95–104. [PubMed: 22803011]
23. RAPUANO BE, SINGH H, BOSKEY AL, DOTY SB, MACDONALD DE. Effects of heat and radiofrequency plasma glow discharge pretreatment of a titanium alloy : evidence for enhanced osteoinductive properties. J Cell Biochem. 2013; 114:1917–1927. [PubMed: 23494951]
24. DALTON BA, MACFARLAND CD, UNDERWOOD PA, STEELE JG. Role of the heparin-binding domain of fibronectin in attachment and spreading of human bone-derived cells. J Cell Sci. 1995; 108:2083–2092. [PubMed: 7657726]
25. PULEO DA, BIZIOS R. RGDS tetrapeptide binds to osteoblasts and inhibits fibronectin-mediated attachment. Bone. 1991; 12:271–276. [PubMed: 1793678]
26. PULEO DA, BIZIO R. Mechanisms of fibronectin-mediated attachment of osteoblasts in vitro. Bone Miner. 1992; 18:215–226. [PubMed: 1392695]
27. PIERSCHBACHER MD, RUOSLAHTI E. Cell attachment activity of fibronectin can be duplicated by small synthetic fragments of the molecule. Nature. 1984; 309:30–33. [PubMed: 6325925]
28. STUBBS JE 3rd, MINTZ KP, EANES ED, TORCHIA DA, FISHER LW. Characterization of native and recombinant bone sialoprotein: delineation of the mineral-binding and cell attachment domains and structural analysis of the RGD domain. J Bone Miner Res. 1997; 12:1210–1222. [PubMed: 9258751]
29. FLORES ME, NORGARD M, HEINEGARD D, REINHOLT FP, ANDERSSON G. RGD-directed attachment of isolated rat osteoclast to osteopontin, bone sialoprotein, and fibronectin. Exp Cell Res. 1992; 201:526–530. [PubMed: 1639145]
30. ALSBERG E, ANDERSON KW, ALBEIRUTI A, FRANCESCHI RT, MOONEY DJ. Cell-interactive alginate hydrogels for bone tissue engineering. J Dent Res. 2001; 80:2025–2029. [PubMed: 11759015]
31. LUTOLF MP, WEBER FE, SCHMOEKEL HG, SCHENSE JC, KOHLER T, MULLER R, HUBBELL JA. Repair of bone defects using synthetic mimetics of collagenous extracellular matrices. Nat Biotech. 2003; 21:513–518.
32. CORRENTE G, ABUNDO R, CARDAROPOLI D, CARDAROPOLI G, MARTUSCELLI G. Long-term evaluation of osseointegrated implants in regenerated and nonregenerated bone. Int J Periodont Restor Dent. 2000; 20:390–397.
33. ERLI HJ, RUGER M, RAGOSS C, JAHNEN-DECHENT W, HOLLANDER DA, PAAR O, VON WALTER M. The effect of surface modification of a porous TiO2/perlite composite on the ingrowth of bone tissue in vivo. Biomaterials. 2006; 27:1270–1276. [PubMed: 16139880]
34. MACDONALD DE, RAPUANO BE, VYAS P, LANE JM, MEYERS K, WRIGHT T. Heat and radiofrequency plasma glow discharge pretreatment of a titanium alloy promote bone formation and osseointegration. J Cell Biochem. 2013 In Press.
35. FUTAMI T, FUJII N, OHNISHI H, TAGUCHI N, KUSAKARI H, OHSHIMA H, MAEDA T. Tissue response to titanium implants in the rat maxilla: ultrastructural and histochemical observations of the bone-titanium interface. J Periodont. 2000; 71:287–298. [PubMed: 10711620]
36. GRZESIK WJ, IVANOV B, ROBEY FA, SOUTHERLAND J, YAMAUCHI M. Synthetic integrin-binding peptides promote attachment and proliferation of human periodontal ligament cells in vitro. J Dent Res. 1998; 77:1606–1612. [PubMed: 9719034]
37. PIERSCHBACHER MD, RUOSLAHTI E. Influence of stereochemistry of the sequence Arg-Gly-Asp-Xaa on binding specificity in cell attachment. J Biol Chem. 1987; 262:17294–17298. [PubMed: 3693352]
38. VAN DER PLUJIM G, VLOEDGRAVEN HJ, IVANOV B, ROBEY FA, GRZESIK WJ, ROBEY PG, PAPAPOULOS SE, LOWIK CW. Bone sialoprotein peptides are potent inhibitors of breast cancer cell attachment to bone. Cancer Res. 1996; 56:1948–1955. [PubMed: 8620518]

39. BLAESS S, KAMMERER RA, HALL H. Structural analysis of the sixth immunoglobulin-like domain of mouse neural cell attachment molecule L1 and its interactions with alpha(v)beta3, alpha(IIb)beta3, and alpha5beta1 integrins. J Neurochem. 1988; 71:2615–2625. [PubMed: 9832163]
40. COPIE V, TOMITA Y, AKIYAMA SK, AOTA S, YAMADA KM, VENABLE RM, PASTOR RW, KRUEGER S, TORCHIA DA. Solution structure and dynamics of linked cell attachment modules of mouse fibronectin containing the RGD and synergy regions: comparison with the human fibronectin crystal structure. J Mol Biol. 1998; 277:663–682. [PubMed: 9533887]
41. FISHER LW, TORCHIA DA, FOHR B, YOUNG MF, FEDARKO MS. Flexible structures of SIBLING proteins, bone sialoprotein, and osteopontin. Biochem Biophys Res Com. 2001; 280:460–465. [PubMed: 11162539]
42. CHOU PY, FASMAN GD. Conformational parameters for amino acids in helical, beta-sheet and random coil regions calculated from proteins. Biochem. 1974; 13:211–222. [PubMed: 4358939]
43. ROY A, KUCUKURAL A, ZHANG Y. I-TASSER: a unified platform for automated protein structure and function prediction. Nat Protocols. 2010; 5:725–738.
44. ZHANG Y. I-TASSER server for protein 3D structure prediction. BMC Bioinformatics. 2008; 9:40–47. [PubMed: 18215316]
45. LANDEGREN U. Measurement of cell numbers by means of the endogenous enzyme hexosaminidase. Applications to detection of lymphokines and cell surface antigens. J Immunol Methods. 1984; 67:379–388. [PubMed: 6200537]
46. SCHWARTZ Z, LOHMANN CH, OEFINGER J, BONEWALD LF, DEAN DD, BOYAN BD. Implant surface characteristics modulate differentiation behavior of cells in the osteoblastic lineage. Adv Dent Res. 1999; 13:38–48. [PubMed: 11276745]
47. RUOSLAHTI E. RGD and other recognition sequences for integrins. Annu Rev Cell Dev Biol. 1996; 12:697–715. [PubMed: 8970741]
48. ADLER M, WAGNER G. Sequential 1H NMR assignments of kistrin, a potent platelet aggregation inhibitor and glycoprotein IIb-IIIa antagonist. Biochem. 1992; 31:1031–1039. [PubMed: 1734953]
49. DICKINSON CD, VEERAPANDIAN B, DAI XP, HAMLIN RC, XUONG NH, RUOSLAHTI E, ELY KR. Crystal structure of the tenth type III cell attachment module of human fibronectin. J Mol Biol. 1994; 236:1079–1092. [PubMed: 8120888]
50. PETTERSON E, LUNING B, MICK H, HEINEGARD D. Synthesis, NMR and function of an O-phosphorylated peptide, comprising the RGD-attachment sequence of osteopontin. Acta Chem Scand. 1991; 45:604–608. [PubMed: 1764332]
51. KESELOWSKY BG, COLLARD DM, GARCIA AJ. Surface chemistry modulates fibronectin conformation and directs integrin binding and specificity to control cell adhesion. J Biomed Mater Res. 2003; 66A:247–259.
52. RUOSLAHTI E. RGD and other recognition sequences for integrins. Annu Rev Cell Dev Biol. 1996; 12:697–715. [PubMed: 8970741]
53. MIDURA RJ, HASCALL VC. Bone sialoprotein – A mucin in disguise ? Glycobiology. 1996; 6:677–681. [PubMed: 8953277]
54. MINTZ KP, GRZESIK WJ, MIDURA RJ, ROBEY PG, TERMINE JD, FISHER LW. Purification and fragmentation of nondenatured bone sialoprotein: evidence for a cryptic, RGD-resistant cell attachment domain. J Bone Miner Res. 1993; 8:985–995. [PubMed: 8213261]
55. ROSS FP, CHAPPEL J, ALVAREZ JI, SANDER D, BUTLER WT, FARACH-CARSON MC, MINTZ KA, ROBEY PG, TEITELBAUM SL, CHERESH DA. Interactions between the bone matrix proteins osteopontin and bone sialoprotein and the osteoclast integrin alpha v beta 3 potentiate bone resorption. J Biol Chem. 1993; 268:9901–9907. [PubMed: 8486670]
56. VON MARSCHALL Z, FISHER LW. Dentin matrix protein-1 isoforms promote differential cell attachment and migration. J Biol Chem. 2008; 283:32730–32740. [PubMed: 18819913]
57. BYZOVA TV, KIM W, MIDURA RJ, PLOW EF. Activation of integrin αVβ3 regulates cell attachment and migration to bone sialoprotein. Exp Cell Res. 2000; 254:299–308. [PubMed: 10640428]

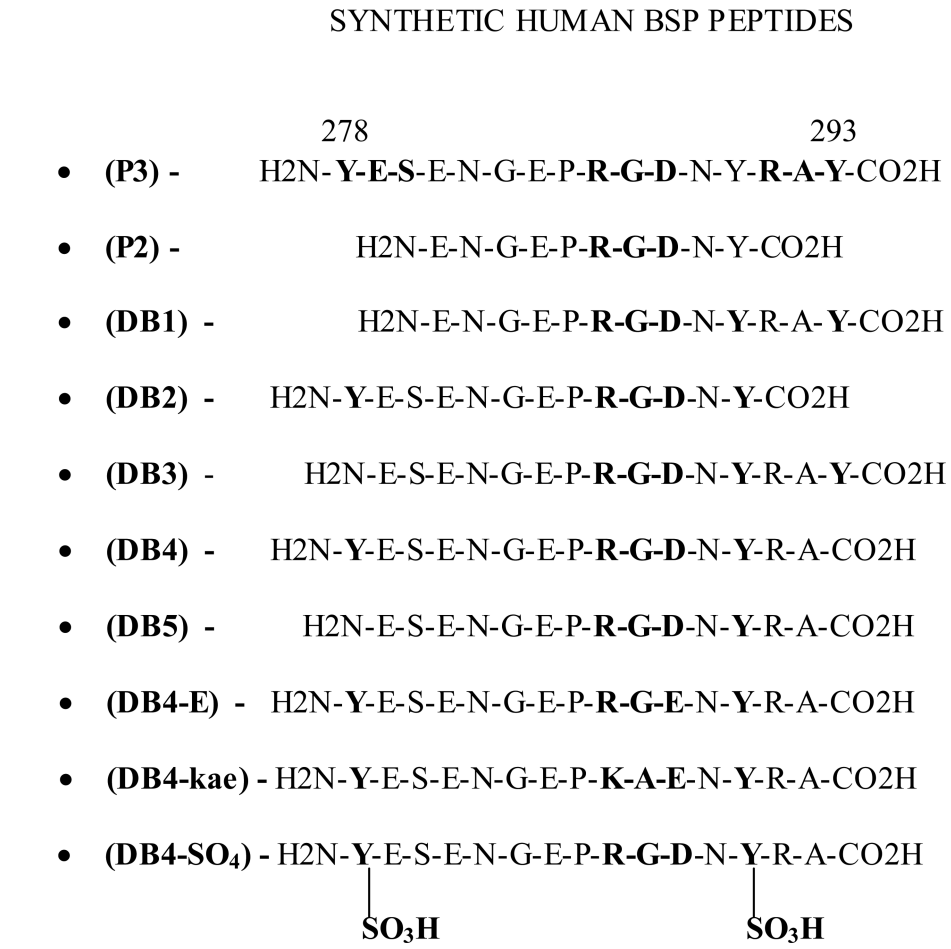

FIGURE 1.

Sequences of human BSP peptides (hBSP). The comparative sequences of BSP residues 278-293 (P3), 281-290 (P2), 281-293 (DB1), 278-290 (DB2), 279-293 (DB3), 278-292 (DB4) and 279-292 (DB5) are shown with the RGD core sequence (286-288) as a reference point. The comparative sequences of two variants of hBSP peptide 278-292 modified within the RGD sequence, including the replacement of aspartic acid with glutamic acid at residue 288 (DB4-E) and the replacement of arg-gly-asp at 286-288 with lys-ala-glu (DB4-KAE) ; and a third peptide modified by the sulfation of tyrosines 278 and 290 (DB4-sulfate), are also shown.

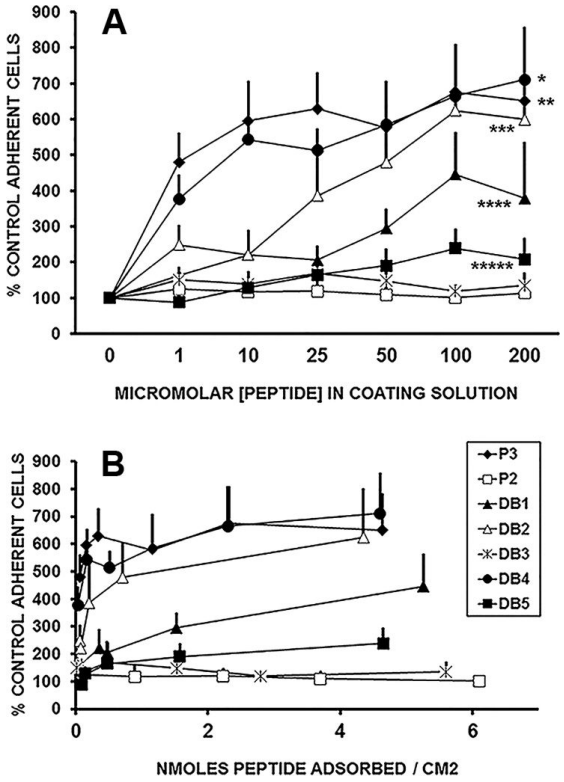

FIGURE 2.

Relative potencies of hBSP peptides P3 and P2, DB1, DB2, DB3, DB4, DB5 for stimulating the attachment of MC3T3 cells. (A) The number of attached cells measured in the wells of nontissue culture plates coated with either peptide as described in Methods is expressed as a percentage of the number of attached cells measured in control wells that were not coated with peptide (control number of attached cells = 2411 ± 13 cells per well; mean ± SEM; N = 9). Data presented as mean ± SEM for control and for each coating concentration of peptide were obtained from at least three independent cell cultures (N = at least 3). *P < 0.001 compared to control and P < 0.04 compared to DB1, DB3, DB5 or P2 at every peptide coating concentration shown based on student's t test. **P < 0.001 or less compared to control. ***P < 0.007 or less compared to control for every concentration tested. ****P < 0.02 or less compared to control for every concentration tested. *****P < 0.02 or less compared to control for peptide coating concentrations (shown on X axis) 25 – 200 uM. (B) For each hBSP peptide, the number of attached cells was also plotted vs. the adsorbed peptide's surface concentration measured by protein assay.

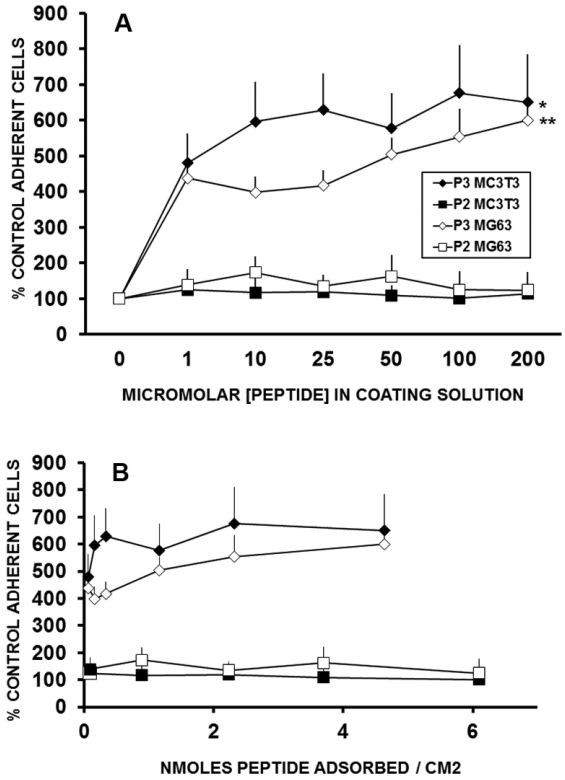

FIGURE 3.

Relative potencies of hBSP peptides P3 and P2 for stimulating the attachment of MC3T3 and MG63 cells. (A) The number of attached cells measured in the wells of nontissue culture plates coated with either peptide as described in Methods is expressed as a percentage of the number of attached cells measured in control wells that were not coated with peptide. The data for attachment of MC3T3 cells to peptides was taken from Fig. 2. For MG63 cells, control number of attached cells = 3624 ± 390 cells per well; mean ± SEM; N = 6. Data presented as mean ± SEM for each peptide coating concentration were obtained from at least three independent cell cultures (N = at least 3). *$P < 0.001$ or less compared to control and $P < 0.04$ compared to P2 at every peptide coating concentration shown based on student's t test. **$P < 0.001$ or less compared to control and $P < 0.05$ compared to P2 at every peptide coating concentration shown based on student's t test. (B) For each hBSP peptide, the number of attached cells was also plotted vs. the adsorbed peptide's surface concentration measured by protein assay.

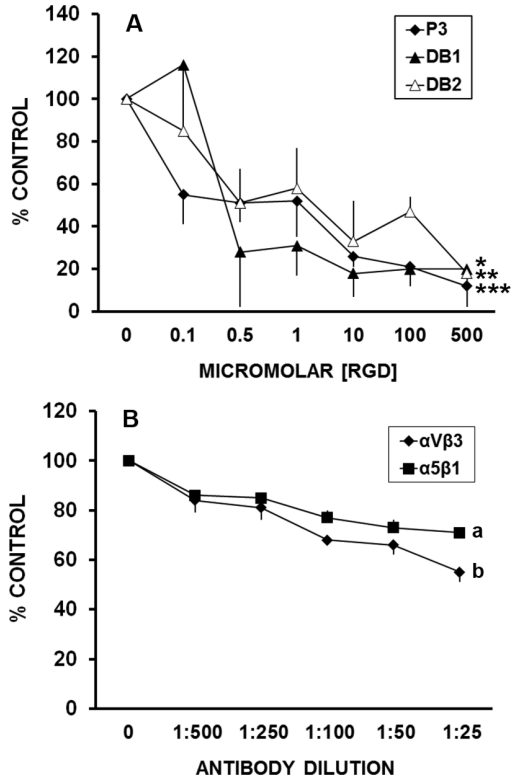

Figure 4.

Inhibitory effects of soluble RGD tripeptide or anti-integrin antibodies on MC3T3 cell attachment to hBSP peptides. The effects of increasing concentrations of soluble (A) RGD or (B) anti-integrin (α_v or $\alpha_5\beta_1$) antibodies, respectively, on the number of MC3T3 cells that attached to (A) P3, DB1 and DB2 (25 μM coating concentration) or (B) peptide P3 (10 μM) were measured. Cells were preincubated with a solution containing 0.1 – 500 μM of the tripeptide RGD or 1:500 to 1:25 dilutions of an anti-α_v or anti-$\alpha_5\beta_1$ integrin antibody for 30 min. prior to addition of cells to the peptide-coated nontissue culture plates. The number of cells that attached to peptide-coated plates measured at each [RGD] or antibody dilution is expressed as a percentage of the control attached cell number (CONTROL) measured when plates were coated with peptides but cells were not preincubated with RGD (0 MICROMOLAR [RGD]) or antibodies (0 ANTIBODY DILUTION). Data are presented as mean ± SEM peptide (N = at least 3). *P < 0.01 or less for RGD concentrations of 100 and 500 μM compared to control (0 μM RGD) - DB1-coated plates. **P < 0.035 or less for RGD concentrations of 100 and 500 μM compared to control (0 μM RGD) - DB2-coated plates. ***P < 0.05 or less for RGD concentrations of 10, 100 and 500 μM compared to control (0 μM RGD) - P3-coated plates. ^{a,b}P < 0.007 or 0.0001, respectively, or less for every dilution of anti-α_v or anti-$\alpha_5\beta_1$ integrin antibodies compared to control (0 ANTIBODY DILUTION) - P3-coated plates (based on student's t test).

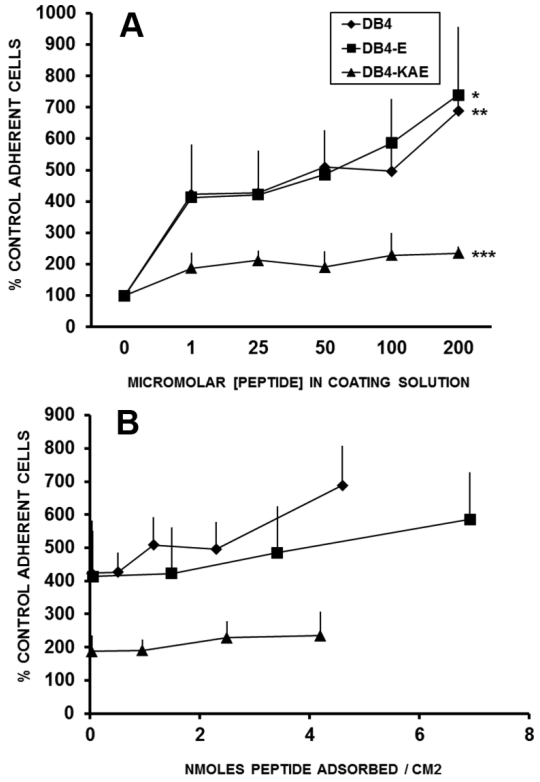

FIGURE 5.

Relative cell attachment potencies of DB4, DB4-E and DB4-KAE. (A) The number of attached cells measured in the wells of nontissue culture plates coated with either peptide is expressed as described under Figure 2 (control number of attached cells = 2803 ± 9 cells per well; mean ± SEM; N = 15). Data presented as mean ± SEM for control and for each coating concentration of peptide were obtained from at least three independent cell cultures (N = at least 3). *P < 0.001 compared to control at every peptide coating concentration shown based on student's t test. **P < 0.006 compared to control at every concentration shown and P < 0.05 compared to DB4-KAE-coated wells at 25 - 200 uM. ***P < 0.003 compared to control at every peptide coating concentration (shown on X axis). (B) For each hBSP peptide, the number of attached cells was also plotted vs. the adsorbed peptide's surface concentration measured by protein assay.

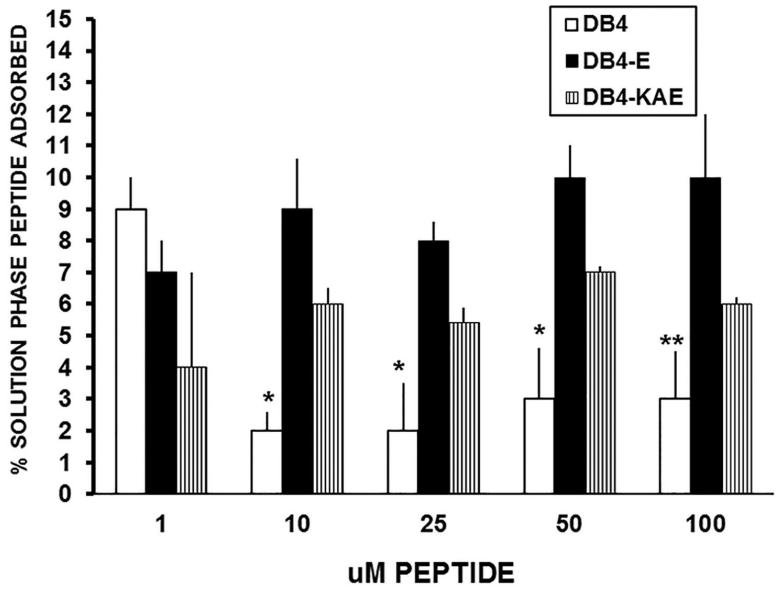

FIGURE 6.

Per cent adsorption of DB4, DB4-E and DB4-KAE to 96-well plates. 96-well nontissue culture plates were coated with peptides and washed as described in Methods. The mean amount of adsorbed peptides measured at coating solution concentrations of 1, 10, 25, 50 and 100 ±M is expressed as % of solution phase peptide in moles (peptides added in solution phase of 200 ul/well) adsorbed to each well. If 100 % of the peptide molecules in a 100 ±M peptide solution adsorbed to the well in a 96-well culture plate, this would correspond to a peptide surface concentration of 70.8 nmoles / cm^2. Data presented as mean ± SEM for control and for each concentration (N = 3-4). *P < 0.04 for 10-50 Fig. μM DB4 compared to DB4-E and DB4-KAE based on student's t test. **P < 0.05 for 100 μM DB4 compared to DB4-E. and DB4-KAE.

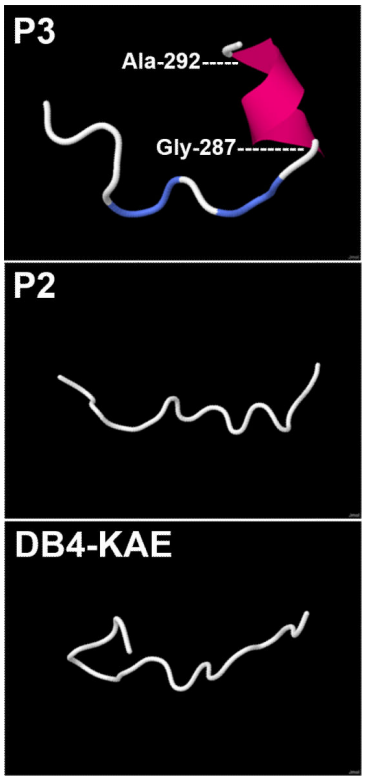

FIGURE 7.

Computer model-generated predictions of hBSP secondary structure. Secondary structures predicted with the aid of the I-Tasser server are shown for peptides P3, P2 and DB4-KAE. Regions of individual peptides predicted to contain an alpha helix secondary structure are shown in red. For peptide models containing areas of alpha helix conformation (P3 and DB3), the relative positions of polar and nonpolar residues outside of the alpha helix structure are shown in blue and grey, respectively. The N-terminus is located on the left-hand side of each of the four models shown.

Table 1

Primary and secondary structures of hBSP peptides in relationship to cell adhesive activity. Amino acid sequence structures favoring alpha helix and beta sheet secondary structures based on computer modeling are shown in red and blue, respectively.

Peptide	Name	Predicted secondary structure of RGD somain favored by its primary structure	RGD sequence	Cell attachment activity
278 293 YESENGEPRGDNYRAY	P3	Helix	RGD	High
ENGEPRGDNY	P2	Coil	RGD	Very low
ENGEPRGDNYRAY	DB1	Helix	RGD	Low
YESENGEPRGDNY	DB2	Coil	RGD	Moderate
ESENGEPRGDNYRAY	DB3	Helix	RGD	Low
YESENGEPRGDNYRA	DB4	Sheet	RGD	High
YESENGEPRGENYRA	DB4-E	Sheet	RGE	High
YESENGEPKAENYRA	DB4-kae	Coil	KAE	Low
ESENGEPRGDNYRA	DB5	Sheet	RGD	Low